ORGANOMETALLICS

Article

Cite This: *Organometallics* 2018, 37, 934−940

Activation of Triphenylphosphine Oxide Mediated by Trivalent Organouranium Species

Caleb J. Tatebe,[†] Zhengjia Tong,[†] John J. Kiernicki, Ezra J. Coughlin, Matthias Zeller, and Suzanne C. Bart*

H. C. Brown Laboratory of Chemistry, Department of Chemistry, Purdue University, West Lafayette, Indiana 47907, United States

Supporting Information

ABSTRACT: Treating a family of uranium benzyl compounds, $Tp^*_2U(CH_2Ph)$ (**1-Bn**), $Tp^*_2U(CH_2\text{-}para\text{-}^iPrPh)$ (**1-^{i}Pr**), $Tp^*_2U(CH_2\text{-}para\text{-}^t BuPh)$ (**1-^{t}Bu**), or $Tp^*_2U(CH_2\text{-}meta\text{-}OMePh)$ (**1-OMe**), which are supported by two hydrotris(3,5-dimethylpyrazolyl)borate (Tp*) ligands, with a single equivalent of triphenylphosphine oxide ($OPPh_3$) causes a unique carbon−carbon coupling to occur. The products of this reaction, $Tp^*_2U[OP(C_6H_5)_2(C_6H_5CH_2C_6H_5)]$ (**2-Ph**), $Tp^*_2U[OP(C_6H_5)_2(C_6H_5CH_2\text{-}p\text{-}iPrC_6H_4)]$ (**2-^{i}Pr**), $Tp^*_2U[OP(C_6H_5)_2(C_6H_5CH_2\text{-}p\text{-}tBuC_6H_4)]$ (**2-^{t}Bu**), and $Tp^*_2U[OP(C_6H_5)_2(C_6H_5CH_2\text{-}m\text{-}OCH_3C_6H_4)]$ (**2-OMe**), are characterized by coupling between the benzyl substituent and the *para*-carbon of one of the phenyl groups of $OPPh_3$. To probe the scope of this unusual reactivity, **1-Bn** was treated with different tris(aryl)phosphine oxides, including tris(*p*-tolyl)phosphine oxide, which yields $Tp^*_2U[OP(p\text{-tolyl})_2(C_6H_4(CH_3)CH_2C_6H_5)]$ (**3-tolyl**). All compounds were characterized by multinuclear NMR, vibrational, and electronic absorption spectroscopies. When possible, X-ray diffraction was used to confirm molecular structures.

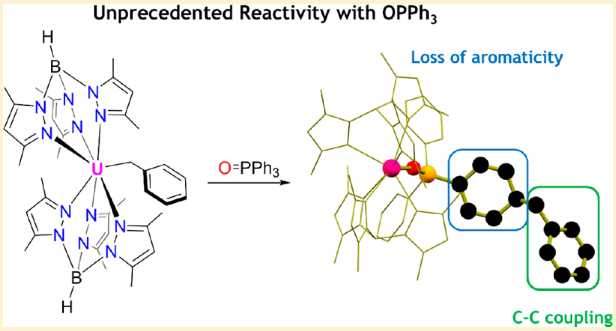

INTRODUCTION

Triphenylphosphine oxide is a popular ligand in coordination chemistry, as its sterically accessible oxygen atom and large size make it ideal for coordinating to electropositive metals.[1] The crystalline nature of this material is also attractive, often imparting desirable properties to organometallic species to facilitate growth of single crystals suitable for X-ray diffraction analysis.[2] The widespread use of $OPPh_3$ as a ligand is due to its inert nature, making it a supportive spectator while chemistry generally occurs at other reactive sites on the metal. In fact, modification of metal-ligated triphenylphosphine oxide is rare; activation is more commonly noted on the free organic.

The actinides are suitable elements to activate inert molecules such as triphenylphosphine oxide, as they are highly reducing and oxophilic metals. Early actinides in particular regularly perform one-electron chemistry, driven by their available redox couples. This is especially true for uranium, the most studied of all the actinides in organometallic chemistry,[3,4] which has been shown to routinely reduce small, oxygenated organic molecules. Low-valent uranium species in particular have routinely been observed to generate and/or support organic radicals in solution.[5−8] For instance, Meyer and co-workers have demonstrated that treating $[((^{Ad}ArO)_3tacn)U^{III}]$ ($(^{Ad}ArO)_3tacn$ = 1,4,7-tris(3-adamantyl-2-hydroxy-5-*tert*-butylbenzyl)-1,4,7-triazacyclononane) with benzophenone generates a fleeting ketyl radical complex, $[((^{Ad}ArO)_3tacn)U^{IV}(OC{\cdot}Ph_2)]$, that head-to-tail *para*-couples, forming the Gomberg dimer derivative $[((^{Ad}ArO)_3tacn)U^{IV}(OCPhPh\text{−}CPh_2O)U^{IV}((^{Ad}ArO)_3tacn)]$.[9] More recently, the Schelter group reported activation of *N*,*N*-dimethylbenzamide by $U(N(SiMe_3)_2)_3$, which forms tetravalent, charge separated $U[OC{\cdot}(Ph)(NMe_2)][N(SiMe_3)_2]_3$, which features the first stabilized amide radical.[10]

In our laboratory, the sterically bulky hydrotris(3,5-dimethylpyrazolyl)borate (Tp*) ligand framework has been useful in isolating uranium(III) complexes featuring ligand radicals.[7] Treating trivalent $Tp^*_2UCH_2Ph$ (**1-Bn**),[11] which serves as a source of $[Tp^*_2U]$, with an equivalent of benzophenone forms $Tp^*_2U(OC{\cdot}Ph_2)$,[12] which was characterized to contain a uranium(III) ion with one-electron reduced benzophenone. Formation of this species is attributed to the oxophilicity and reducing nature of uranium, which performs an electron transfer after initial benzophenone coordination, creating a strong, anionic U−O bond.[12] The large bis(Tp*) framework prevents further coupling chemistry at the ligand radical, which is in contrast to the observation by Meyer. On the basis of this exciting result, we hypothesized that other oxygenated substrates could be activated in a one-electron process. Herein, we report the reactivity of a series of trivalent uranium benzyl species,[13] both with and without *para*-substitution, with triphenylphosphine oxides. Rather than an isolable ligand radical, coupling of the benzyl group with the *para*-carbon of triphenylphosphine oxide was noted, contrasting our previous

Received: December 17, 2017
Published: March 6, 2018

DOI: 10.1021/acs.organomet.7b00896
Organometallics 2018, 37, 934−940

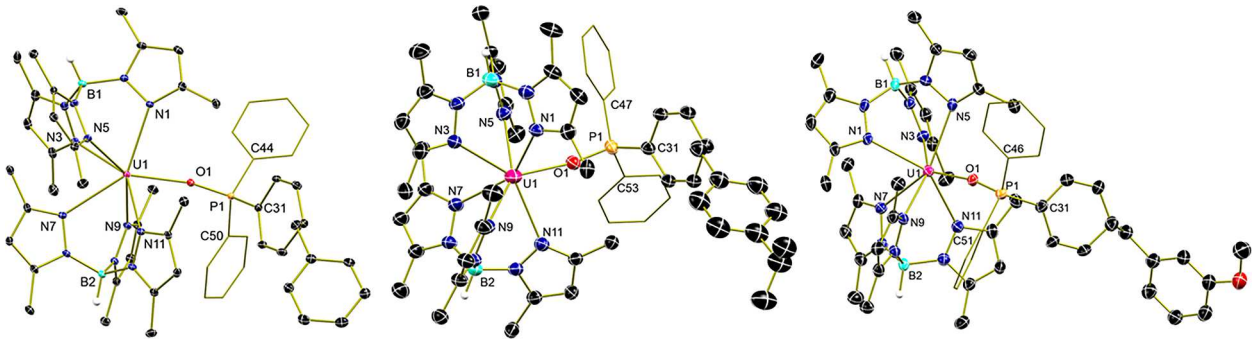

Figure 1. Molecular structure of **2-Ph** (left), **2-^{i}Pr** (middle), and **2-OMe** (right) displayed with 30% probability ellipsoids. Selected hydrogen atoms, ellipsoids, and co-crystallized solvent molecules omitted for clarity (full structures presented in the SI).

results with benzophenone in which the benzyl radical was extruded as bibenzyl. Full spectroscopic and structural characterization has been used to elucidate these interesting new structures from this unusual activation of $OPPh_3$.

RESULTS AND DISCUSSION

Synthesis and Characterization of a Unique Carbon−Carbon Coupled Product, Tp*$_2$U[OP(C$_6$H$_5$)$_2$(C$_6$H$_5$CH$_2$-C$_6$H$_5$)] (2-Ph). To begin our studies, a solution of Tp*$_2$UCH$_2$Ph (**1-Bn**) was charged with an equivalent of $OPPh_3$, causing an immediate color change from green to brown. After 45 min, workup and analysis of the dark brown powder by ^{1}H NMR spectroscopy (25 °C, C_6D_6) revealed a complex, paramagnetically shifted spectrum, with no resonances for either starting material, indicating complete conversion to a new compound.

Due to the complexity of this ^{1}H NMR spectrum, structural assignment of this brown compound by X-ray diffraction was sought. Analysis of crystals obtained by slow diffusion of *n*-pentane into a concentrated toluene solution at −35 °C revealed the product as Tp*$_2$U[OP(C$_6$H$_5$)$_2$(C$_6$H$_5$CH$_2$C$_6$H$_5$)] (**2-Ph**) (Figure 1, left; eq 1; Figure 2), which features a

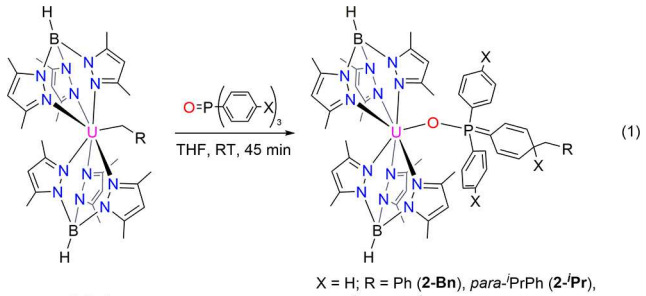

1-Bn'

X = H; R = Ph (**2-Bn**), *para*-^{i}PrPh (**2-^{i}Pr**), *para*-^{t}BuPh (**2-^{t}Bu**), *meta*-OMePh (**2-OMe**)
X = CH_3 (**3-tolyl**); R = Ph

carbon−carbon bond between the benzyl group and the carbon at the *para*-position of one of the phenyl rings of $OPPh_3$. In addition to the new C−C bond, an elongation of the P═O bond and a new U−O bond are observed. The U−$N_{pyrazole}$ bond lengths for the pair of κ^3-Tp* ligands range from 2.529(3) to 2.744(3) Å, which is consistent with other U−$N_{pyrazole}$ bond lengths for bis(Tp*)U(III) compounds.[23,28,29] The U−O bond distance (2.358(2) Å) is significantly longer than other anionic U(III)−O bond lengths (2.144−2.271 Å, Table 1) and is closer to that of neutral U−O bond distances (2.350−2.584 Å, Table 1). We postulate this is an anionic interaction but extreme

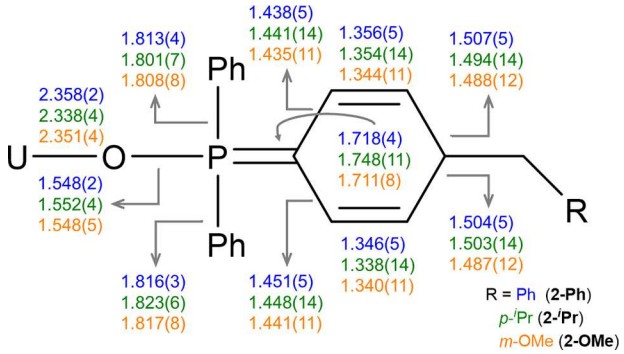

Figure 2. Selected bond lengths of **2-Ph**, **2-^{i}Pr**, and **2-OMe**.

steric hindrance at the uranium center creates the observed elongation.

To investigate this hypothesis, we sought to synthesize a similarly crowded uranium center with a U−O neutral bond. Treating a THF solution of **1-Bn** with BPh_3 affords a blue powder assigned as [Tp*$_2$U(THF)][BnBPh$_3$] (**4-THF**) (see the Supporting Information for full details). The molecular structure of **4-THF** as determined by X-ray diffraction of single crystals revealed a bis(Tp*)U cation with a coordinated THF molecule, as well as a $BnBPh_3$ counteranion. The U−O bond distance of 2.609(3) Å is significantly longer than that for **2-Ph**, confirming assignment of the latter as an anionic U−O interaction (Figure S1).

Further analysis of the structural parameters of **2-Ph** (Figure 2) highlight distortions in the triphenylphosphine oxide ligand. Comparison of the O−P bond length (1.548(2) Å) in **2-Ph** to those of coordinated phosphine oxide ligands in low-valent uranium complexes shows clear P═O bond reduction (Tp*UCl$_3$(OP(OC$_2$H$_5$)$_3$) = 1.44(1) Å;[25] Cp′$_3$U(OPPh$_3$) (Cp′ = η^5-MeC$_5$H$_4$) = 1.492(6) Å).[26] Examination of the P−C bond lengths shows two distinct bonding modes. For the phenyl ring that has undergone *para*-carbon coupling, the distance is shortened (P1−C31 = 1.718(4) Å) compared to the other two (P1−C44 = 1.816(3), P1−C50 = 1.813(4) Å). The latter distances are similar to that observed for Cp′$_3$U(OPPh$_3$) (1.794(6)−1.799(8) Å),[26] which has a neutral $OPPh_3$ coordinated to a trivalent uranium center. This shortened P−C bond distance results from reduction of the adjacent O−P bond and has not been previously observed for uranium compounds.

With these distortions noted in the O−P−C bonds for **2-Ph**, similarly the adjacent phenyl ring also displays unusual parameters; most notably, the ring has undergone a loss of

DOI: 10.1021/acs.organomet.7b00896
Organometallics 2018, 37, 934−940

Table 1. U−O Bond Comparison for U(III) Complexes'''

Compound (red = anionic; blue = neutral)	Bond Length (Å)
2-Ph	2.358(2)
$U(ODtbp)_3$ ($ODtbp = OC_6H_3$-Bu^t_2-2,6)	2.151(3)-2.164(3)[17]
$U(OAr^{Ad,Ad,Me})_3$ ($OAr^{Ad,Ad,Me}$ = O-C_6H_2-2,6-Ad-4-Me)	2.151(3)-2.177(3)[18]
{Cp*[2,6-$(Me_3C)_2$-4-Me-C_6H_2O]U}$_2$(C_6H_6)	2.144(8)[19]
((ArO_3)tacn)U($NCCH_3$) (ArO_3(tacn) = 1,4,7-tris(3,5-di-*tert*-butyl-2-hydroxybenzyl)-1,4,7-triazacyclononane)	2.258(5)-2.271(5)[20]
$Tp^*_2U[OC(CH_3)CH_2]$	2.198(9)[21]
$Tp^{Ph}UI(OPh)(THF)_2$ (Tp^{Ph} = hydrotris(3-phenylpyrazolyl)borate)	2.184(2)[22]
$Tp^*_2U(O$-C_6H_3-2,4,6-Me)	2.159(10)[23]
$Tp^{iPr2}UI_2(OPPh_3)$ (Tp^{iPr2} = hydrotris(3,5-di-*iso*-propylpyrazolyl)borate)	2.350(11)[24]
$Tp^*UCl_3[OP(OC_2H_5)_3]$	2.373(7)[25]
$Cp'_3U(OPPh_3)$ ($Cp' = \eta^5$-MeC_5H_4)	2.389(6)[26]
$UI_2\{H(\mu$-$H)B(3$-^{t}Bu,5-Me-$pz)_2\}(OPPh_3)_2$	2.584(12)[27]
4-THF	2.609(3)

aromaticity. The C−C bond distances display a pattern indicative of a cyclohexadienyl fragment (Figure 2) rather than an aromatic system. A recent report by Schelter et al. shows this same loss of aromaticity from dimeric coupling of a uranium tris(amide) complex featuring a benzophenone radical to afford $[N(SiMe_3)_2]_3U(OCPhPh$-CPh-$CPh_2O)U[N(SiMe_3)_2]_3$.[10] Keay reports loss of aromaticity in a phenyl ring of a triphenylphosphine oxide derivative can be facilitated by LDA (LDA = lithium diisopropylamide), forming a bicyclic triene.[30]

The structural assignment of **2-Ph** provided insight into the complex solution ^{1}H NMR spectrum (Table 2). Thirteen resonances were observed ranging from −16 to 22 ppm, consistent with a C_s symmetric spectrum. Three resonances were observed for Tp* ligands, assignable to the *endo*- and *exo*-methyl groups and the pyrazole CH consistent with this symmetry assignment. The unmodified phenyl rings on the triphenylphosphine ligand show three resonances for the *para*, *meta*, and *ortho* protons (10.51, 21.72, 10.78 ppm, respectively). For the modified phenyl ring, two singlets (2H each) are assigned as the cyclohexadienyl resonances, and this was additionally confirmed by 2D ^{1}H NMR correlation spectroscopy (COSY) (Figure S6). The protons for the benzyl substituent for **2-Ph** are not paramagnetically shifted, likely due to their distance from the uranium. A broad singlet appearing at 8.37 ppm is assigned as the B-H of Tp*. There is a

Table 2. Selected Spectroscopic Data for 2-Ph, 2-^{i}Pr, 2-^{t}Bu, and 2-OMe

	2-Ph	2-^{i}Pr	2-^{t}Bu	2-OMe
Tp*-CH_3 (endo) (ppm)	−16.06	−16.12	−16.06	−16.04
Tp*-CH_3 (exo) (ppm)	0.61	0.62	0.62	0.61
Tp*-CH (ppm)	7.45	7.45	7.44	7.44
cyclohexadienyl-CH (ppm)	5.40, 15.15	5.42, 15.20	5.41, 15.48	5.44, 15.16
coupled-CH_2 (ppm)	1.91	1.94	1.98	1.99
^{11}B (ppm)	7.2	7.1	6.8	7.4
^{31}P (ppm)	84.77	83.78	83.28	84.71
IR: ν_{BH} (cm^{-1})	2553, 2526	2552, 2524	2550, 2519	2552, 2524

corresponding resonance at 7.2 ppm in the ^{11}B NMR spectrum, which is within the range of other bis(Tp*) U(III) complexes.[31,32] A single resonance appears in the ^{31}P NMR spectrum at 84.77 ppm, which is significantly shifted from $OPPh_3$ (25.74 ppm, Figure S29). The coordination of two κ^3-Tp* ligands was also confirmed by IR spectroscopy (KBr pellet) with two B-H stretches (2553, 2526 cm^{-1}), common for bis(Tp*)U complexes.[12,21,33]

Electronic absorption spectroscopy was utilized to further characterize the oxidation state and color of **2-Ph** (Figure 3).

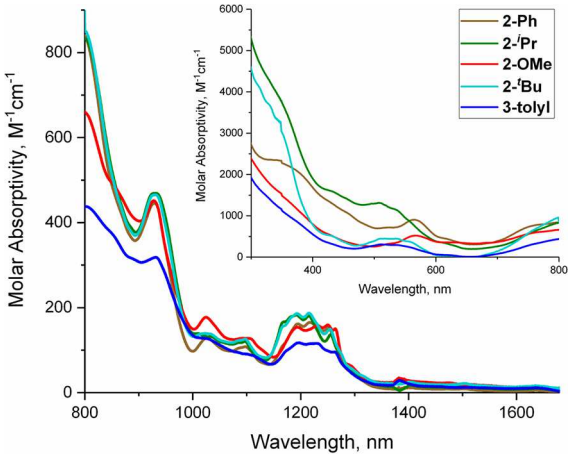

Figure 3. Electronic absorption spectra of **2-Ph** (brown), **2-^{i}Pr** (green), **2-^{t}Bu** (light blue), **2-OMe** (red), and **3-tolyl** (dark blue) recorded from 350 to 1680 nm in THF at ambient temperature.

The near-infrared (NIR) region shows features characteristic of trivalent uranium at 1200 nm (200 M^{-1} cm^{-1}) (Figure 3), which are also observed for **1-Bn**.[11] An absorbance in the UV−visible region with λ_{max} at 565 nm (905 M^{-1} cm^{-1}) is responsible for the brown color observed for **2-Ph**.

Variation of Uranium Benzyl. With full characterization of **2-Ph**, we sought to understand how steric and electronic variation of the benzyl substituents influenced the observed coupling chemistry. To this end, we employed previously reported $Tp^*_2U(CH_2$-*p*-*i*PrPh) (**1-^{i}Pr**), $Tp^*_2U(CH_2$-*p*-*t*BuPh) (**1-^{t}Bu**), and $Tp^*_2U(CH_2$-*m*-OMePh) (**1-OMe**) in our study.[13] Following the same procedure to make **2-Ph**, treating a stirring solution of either **1-^{i}Pr**, **1-^{t}Bu**, or **1-OMe** with $OPPh_3$ forms $Tp^*_2U[OP(C_6H_5)_2(C_6H_5CH_2$-*p*-$CH(CH_3)_2Ph)]$ (**2-^{i}Pr**), $Tp^*_2U[OP(C_6H_5)_2(C_6H_5CH_2$-*p*-$C(CH_3)_3Ph)]$ (**2-^{t}Bu**), and $Tp^*_2U[OP(C_6H_5)_2(C_6H_5CH_2$-*m*-$OCH_3Ph)]$ (**2-OMe**) (eq 1), respectively, as brown powders. Overall, *para*-substitution

DOI: 10.1021/acs.organomet.7b00896
Organometallics 2018, 37, 934−940

slows the reaction rate, but does not prevent the C−C coupling.

All three of these compounds show ^{1}H NMR spectra that are analogous to that of **2-Ph**. Diagnostic peaks corresponding to the Tp* ligands and phenyl rings appear in the range from −16.06 to 21.80 ppm (Table 2). The cyclohexadienyl peaks were confirmed by COSY, and the chemical shifts are akin to those observed for **2-Ph** (Figure S11: **2-^{i}Pr**; Figure S20: **2-OMe**). Similar to **2-Ph**, the protons for the coupled phenyl ring all appear in the diamagnetic region of the ^{1}H NMR spectrum as expected. For **2-^{i}Pr** and **2-^{t}Bu**, two resonances (2H each) for the *meta* and *ortho* protons of the coupled benzyl fragment are seen (**2-^{i}Pr**: 6.12, 6.24 ppm; **2-^{t}Bu**: 6.18, 6.42 ppm), whereas four are observed for **2-OMe** (5.84, 6.08, 6.17, 6.30 ppm; 1H each). The substituted functional groups of **2-^{i}Pr** ($CH(CH_3)_2$ = 0.62 ppm; $CH(CH_3)_2$ = 2.16 ppm), **2-^{t}Bu** ($C(CH_3)_3$ = 0.72 ppm), and **2-OMe** (OCH_3 = 2.64 ppm) show little shift as compared to their diamagnetic reference value in their respective ^{1}H NMR spectra, likely due to their distance from the paramagnetic uranium center. Continued analysis by heteroatom NMR spectroscopy and infrared spectroscopy of this series is consistent with what was observed for **2-Ph** (Table 2). Two B-H stretches are observed by IR spectroscopy (KBr pellet), which is also seen with **2-Ph** (Table 2).

Further characterization of **2-^{i}Pr**, **2-^{t}Bu**, or **2-OMe** by electronic absorption spectroscopy (Figure 3) showed weak absorbances near 1200 nm (ca. 200 M^{-1} cm^{-1}), as with the spectrum of **2-Ph**. The UV−visible region for the substituted family of products displays a broad absorbance in the region 475−600 nm.

To examine the unique coupled products further, a structural comparison of **2-^{i}Pr** and **2-OMe** was made using single crystal X-ray crystallography (Figures 1 and 2). Similar to **2-Ph**, these compounds show 7-coordinate uranium centers with pentagonal bipyramidal geometries. Both display U−$N_{pyrazole}$ distances in the same range as **2-Ph** (**2-^{i}Pr**: 2.541(5)−2.699(5) Å; **2-OMe**: 2.531(6)−2.728(6) Å). The U−O bond lengths (**2-^{i}Pr**: 2.338(4) Å; **2-OMe**: 2.351(4) Å) are on the order of those of **2-Ph**, influenced by the steric pressure of the Tp* ligands. The P−O distance (**2-^{i}Pr** = 1.552(4) Å; **2-OMe**: 1.548(5) Å) is within error of that in **2-Ph**. A similar trend in bonding is seen for the P−C bonds in these two compounds, where the P−$C_{cyclohexadienyl}$ bond lengths (**2-^{i}Pr** = 1.748(11) Å; **2-OMe**: 1.711(8) Å) are shorter than the P−C_{Ph} bond lengths (**2-^{i}Pr** = 1.801(7), 1.823(6) Å; **2-OMe**: 1.808(8), 1.817(8) Å). The distances in the cyclohexadienyl fragment in **2-^{i}Pr** and **2-OMe** are similar to those in **2-Ph** (Figure 2).

Attempts to extend the chemistry beyond benzyl groups were unsuccessful. Treating $Tp^*_2U(CH_2\text{-}ortho\text{-}C_5H_4N)$,[13] which features aza-allyl coordination through the picoline ring, with $OPPh_3$ did not result in the desired coupling chemistry. This is likely due to the aza−allyl coordination mode that does not facilitate benzyl radical formation and dissociation. Similarly, subjecting $Tp^*_2U(CH_2SiMe_3)$[34] to the same reaction conditions that generated **2-Ph** yielded no coupled product, but rather decomposition due to the lack of radical stabilization from the neosilyl group.

Next, the reactivity of $OPPh_3$ was explored for bis(Tp*)U compounds that are established to contain ligand radicals. Surprisingly, no coupled products were observed when treating either $Tp^*_2U(2,2'\text{-bpy})$[7] or $Tp^*_2U(OC{\cdot}Ph_2)$[12] with $OPPh_3$. In either case, no reaction was observed.

Variation of Organic Reagent. To study the effects of altering the electronics of the phosphine oxide, compound **1-Bn** was treated with a family of tris(aryl)phosphine oxides. Using tris(*p*-tolyl)phosphine oxide under the same experimental conditions afforded a brown powder with a paramagnetically shifted ^{1}H NMR spectrum similar to that of **2-Ph**. This compound was isolated, characterized, and assigned as $Tp^*_2U[OP(p\text{-}CH_3C_6H_4)_2\text{-}p\text{-}CH_3C_6H_4CH_2C_6H_5]$ (**3-tolyl**). Multinuclear NMR and IR spectroscopies were also consistent with **2-Ph**. The electronic absorption spectrum of **3-tolyl** trends well with the previously discussed compounds in both the NIR and UV−visible regions (Figure 3). This reaction was markedly slower than the initial benzyl reaction to give **2-Ph**; a color change was not seen until 25 min of stirring with a total reaction time of 85 min.

Variation of the *para*-substituent on the triphenylphosphine oxide with heteroatom containing groups, including $-CF_3$ and −OMe, led to mixtures of products resulting from C−F[32] and C−O activation, respectively, pointing to the fluoro- and oxophilicity of low-valent uranium. Likewise, using DMSO, Ph_2SO, or $OAsPh_3$ in lieu of triphenylphosphine oxides causes instantaneous conversion to previously reported Tp^*_2UO.[35] The sulfur analogue of $OPPh_3$, $SPPh_3$, does not react with **1-Bn** at all. These reactions highlight that the oxophilicities of both phosphorus and uranium are driving forces for the coupling reaction.[36] When tris(p-$N(Me)_2C_6H_4$)phosphine oxide is stirred with **1-Bn**, a complicated mixture of paramagnetic products is seen by ^{1}H NMR spectroscopy, with no evidence for the characteristic coupling product. No reaction between HMPA (HMPA = hexamethylphosphoramide) and **1-Bn** occurs, which may be due to the difference in reduction potentials or the lack of a location to stabilize a ligand radical to promote coupling.

Mechanistic Considerations. Experiments were performed to gain insight into the potential mechanism of the observed coupling chemistry. Using an excess of the hydrogen atom donors 1,4-cyclohexadiene or 9,10-dihydroanthracene in the synthesis of **2-Ph** produced no alteration in the ^{1}H NMR spectra, indicating no H-atom radical abstraction had occurred in either case. Next, the synthesis of **2-Ph** was performed at low temperature (−35 °C), which suspended its formation; production of **2-Ph** is seen upon warming to room temperature. Importantly, during the synthesis of **2-Ph** under any conditions, neither toluene nor bibenzyl was observed by ^{1}H NMR spectroscopy. This supports that benzyl radical coupling to the *para*-carbon of triphenylphosphine oxide is faster than respective H-atom abstraction or homocoupling.

With these experimental outcomes, there are several mechanistic pathways that could be considered. One hypothesis for the mechanism is that, upon addition of $OPPh_3$ to a solution of **1-Bn**, $OPPh_3$ association with the uranium(III) center aides benzyl radical loss due to steric congestion. In concert, a putative $[Tp^*_2U]$ fragment reduces $OPPh_3$ by one electron, which resonates around the phenyl ring to the *para*-position, where it reacts with the extruded benzyl radical, forming the coupled product. Reduction of the P=O bond converts the U−O bond from neutral to anionic, allowing for the formation of the thermodynamically favored U−O anionic bond. If benzyl radical loss happened prior to phosphine oxide coordination, it would be expected to observe decomposition of **1-Bn** in the presence of no substrate, which is not substantiated in a control experiment. The lack of bibenzyl or toluene formation from the reactions supports that the benzyl radical

DOI: 10.1021/acs.organomet.7b00896
Organometallics 2018, 37, 934−940

does not leave the coordination sphere during the course of the reaction.

An alternative pathway is that homolytic scission of the U−C bond takes place *after* the U−O anionic bond formation with incoming $OPPh_3$. This step would give rise to a transient U(IV) intermediate, $Tp^*_2U(CH_2Ph)OPPh_3$, which would get reduced back to U(III) after U−C homolytic scission. This is not favored as there are no examples of $Tp^*_2U(IV)$ complexes being reduced to $Tp^*_2U(III)$ in the absence of strong alkali metal reductant. Furthermore, previously reported Tp*U(NMes)(CH_2Ph)(THF), which features a uranium(IV)−benzyl bond, is stable and fully characterized, showing no proclivity for a homolytic U−C scission and reduction back to uranium(III).[37]

CONCLUSIONS

In summary, we have shown here that the uranium(III) benzyl series, $Tp^*_2UCH_2Ph$ (**1-Bn**), once again participates in radical chemistry. In this case, activation of triphenylphosphine oxides was noted, followed by an unusual coupling reaction at the *para*-position of the phenyl groups. Steric and electronic variation of the benzyl group does not affect the coupling chemistry greatly; however, using a group that does not stabilize a radical intermediate shuts down the observed coupling. Furthermore, using a triphenylphosphine oxide that is substituted at the *para*-position does not prevent the coupling; it only slows the rate, demonstrating the strong driving force for the reaction.

While the overall carbon−carbon coupling is a surprising result, the proposed mechanism is composed of fundamental steps typically observed for uranium in the Tp* system, including single electron transfer, formation of a strong uranium−oxygen bond, and extrusion of benzyl radicals. Specific to this particular set of reactions is the fact that the benzyl radical has an accessible place to couple (at the reduced triphenylphosphine oxide), rather than with itself, which is often observed in this system. Furthermore, reactivity of the triphenylphosphine oxides in this system is noteworthy, given that this family is generally used as inert ligands in coordination chemistry. Such a coupling reaction has not been previously observed for other metals on the periodic table, speaking to the unparalleled reactivity of the actinides in organometallic chemistry.

EXPERIMENTAL SECTION

General Considerations. All air- and moisture-sensitive manipulations were performed using standard Schlenk techniques or in an MBraun inert atmosphere drybox with an atmosphere of purified nitrogen. The MBraun drybox is equipped with a cold well designed for freezing samples in liquid nitrogen as well as two −35 °C freezers for cooling samples and crystallizations. Solvents for sensitive manipulations were dried and deoxygenated based on literature procedures using a Seca solvent purification system.[14] Benzene-d_6 was purchased from Cambridge Isotope Laboratories, dried with molecular sieves and sodium, and degassed by three freeze−pump−thaw cycles. 1,4-Cyclohexadiene, 9,10-dihydroanthracene, triphenylphosphine oxide (Sigma-Aldrich), and triphenylborane (Alfa Aesar) were purchased fromcommercial sources. 1,4-Cyclohexadiene was degassed by three freeze-pump-thaw cycles before use. 9,10-Dihydroanthracene was sublimed before use. Triphenylborane was used as received; triphenylphosphine oxide was dried before use. Benzylpotassium salts,[15] Tp^*_2UBn (**1-Bn**),[11] $Tp^*_2U(CH_2$-*para*-*i*PrPh) (**1-*i*Pr**),[13] $Tp^*_2U(CH_2$-*para*-*tert*-butylphenyl) (**1-^{t}Bu**),[13] and $Tp^*_2U(CH_2$-*meta*-methoxyphenyl) (**1-OMe**)[13] were prepared per literature procedures. Substituted tris(aryl)phosphine oxides were made with an adaptation of a literature procedure.[16]

^{1}H NMR spectra were recorded on a Varian Inova 300 spectrometer with an operating frequency of 299.992 MHz. All chemical shifts are reported relative to the peak for $SiMe_4$, using 1H (residual) chemical shifts of the solvent (C_6D_6: 7.16 ppm) as a secondary standard. ^{11}B chemical shifts are reported relative to the peak for $BF_3{\cdot}Et_2O$ (0.0 ppm). ^{11}B NMR spectra were recorded on a Varian Inova 300 spectrometer operating at a frequency of 96.24 MHz. ^{31}P NMR spectra were recorded on a Mercury 300 spectrometer operating at a frequency of 121.43 MHz. ^{31}P chemical shifts are reported relative to the peak for 85% H_3PO_4 in C_6D_6 (0.0 ppm). The spectra for paramagnetic molecules were obtained by using an acquisition time of 0.5 s; thus the peak widths reported have an error of ±2 Hz. For paramagnetic molecules, the ^{1}H NMR data are reported with the chemical shift, followed by the peak width at half height in hertz or multiplicity, the integration value, and, where possible, the peak assignment. Pulse-field gradient COSY spectra were obtained using a Bruker AV-III-HD spectrometer with a 5 mm Z-gradient BBFO probe with an operating frequency at 400.17 MHz. Spectra were acquired using 20000 Hz sweep widths in both dimensions. In F2, 4 scans per increment using 4096 data points and a relaxation delay of 1 s. In F1, 8 increments were acquired. The raw data were Fourier transformed into a final data matrix consisting of 4K points in F2 and 2K points in F1. Elemental analyses were performed by Midwest Microlab, LLC (Indianapolis, IN). Solid state infrared spectra were recorded using a Thermo Nicolet 6700 spectrophotometer; samples were made by crushing the solids, mixing with dry KBr, and pressing into a pellet. Electronic absorption spectroscopic measurements were recorded at ambient temperature in sealed 1 cm quartz cuvettes with a Cary 6000i UV−vis−NIR spectrophotometer.

Single crystals of **2-^{i}Pr** and **2-OMe**, suitable for X-ray diffraction, were coated with poly(isobutylene) oil in a drybox and quickly transferred to the goniometer head of a Bruker AXS D8 Quest diffractometer with kappa geometry, an I-μ-S microsource X-ray tube, a laterally graded multilayer (Goebel) mirror single crystal for monochromatization, a Photon2 CMOS area detector, and an Oxford Cryosystems low temperature device. Examination and data collection were performed with Cu Kα radiation (λ = 1.54184 Å). Single crystals of **2-Ph** suitable for X-ray diffraction were transferred to the goniometer head of a Bruker AXS ApexII CCD diffractometer with a sealed tube fine focus X-ray tube and an Oxford Cryosystems low temperature device. Examination and data collection were performed with Mo Kα radiation (λ = 0.71073 Å). Single crystals of **4-THF** suitable for X-ray diffraction were transferred to the goniometer head of a Rigaku Rapid II image plate diffractometer equipped with a MicroMax002+ high intensity copper X-ray source with confocal optics. Preliminary examination and data collection were performed with Cu Kα radiation (λ = 1.54184 Å). Detailed discussion regarding single crystal determinations are available in the Supporting Information. Complete data has been deposited with the CCDC (CCDC 1587804, 1587807, 1587812, 1587813).

Warning! *Depleted uranium (^{238}U) is a weak alpha emitter with a half-life $t_{1/2} = 4 \times 10^9$ years. All manipulations were executed in an inert atmosphere glovebox in a laboratory equipped with proper detection equipment.*

Synthesis of $Tp^*_2U[OP(C_6H_5)_2(C_6H_5CH_2R)]$ (2-R). A 20 mL scintillation vial was charged with Tp^*_2U alkyl (**1-Bn**: 0.300 g, 0.325 mmol; **1-^{i}Pr**: 0.351 g, 0.363 mmol; **1-^{t}Bu**: 0.100 g, 0.102 mmol; **1-OMe**: 0.200 g, 0.208 mmol) in 7 mL of THF. In a separate vial, 1 equiv of $OPPh_3$ (**1-Bn**: 0.090 g, 0.324 mmol; **1-^{i}Pr**: 0.101 g, 0.363 mmol; **1-^{t}Bu**: 0.028 g, 0.102 mmol; **1-OMe**: 0.058 g, 0.208 mmol) was dissolved in 3 mL of THF. The $OPPh_3$ solution was added to the stirring alkyl solution. A color change from green to brown was observed (**2-Ph**: 5 min; **2-^{i}Pr**: 15 min; **2-^{t}Bu**: 30 min; **2-OMe**: 5 min). After additional stirring (**2-Ph**: 40 min; **2-^{i}Pr**: 35 min; **2-^{t}Bu**: 60 min; **2-OMe**: 35 min), volatiles were removed *in vacuo*, leaving a brown powder. Washing with *n*-pentane (3 × 5 mL) and drying afforded brown powders identified as $Tp^*_2U[OP(C_6H_5)_2(C_6H_5CH_2C_6H_5)]$ (**2-Ph**) (0.368 g, 0.306 mmol, 94%), $Tp^*_2U[OP(C_6H_5)_2(C_6H_5CH_2$-*p*-

DOI: 10.1021/acs.organomet.7b00896
Organometallics 2018, 37, 934−940

*i*PrC$_6$H$_4$)] (**2-^{i}Pr**) (0.397 g, 0.319 mmol, 87%), Tp*$_2$U[OP(C$_6$H$_5$)$_2$-(C$_6$H$_5$CH$_2$-*p*-*t*BuC$_6$H$_4$)] (**2-^{t}Bu**) (0.102 g, 0.080 mmol, 80%), and Tp*$_2$U[OP(C$_6$H$_5$)$_2$(C$_6$H$_5$CH$_2$-*m*-OCH$_3$C$_6$H$_4$)] (**2-OMe**) (0.249 g, 0.202 mmol, 96%). Single X-ray quality crystals of **2-Ph** and **2-^{i}Pr** were obtained from a concentrated toluene solution layered with pentane stored at −35 °C. Single X-ray quality crystals of **2-OMe** were obtained from the diffusion of hexamethyldisiloxane into a concentrated toluene solution. **2-Ph**: Elemental analysis of $C_{55}H_{66}B_2N_{12}OPU$, Calculated: C, 54.97; H, 5.54; N, 13.99. Found: C, 54.59; H, 5.52; N, 13.89. ^{1}H NMR (C$_6$D$_6$, 25 °C): δ (ppm) = −16.06 (58, 18H, Tp*-C*H*$_3$), 0.61 (6, 18H, Tp*-C*H*$_3$), 1.91 (6, d, 2H, benzyl-C*H*$_2$), 5.40 (16, 2H, cyclohexadiene-C*H*), 6.16 (d, 2H, benzyl-*o*/*m*-C*H*, *J* = 5.8 Hz), 6.37 (d, 2H, benzyl-*o*/*m*-C*H*, *J* = 6.4 Hz), 7.01 (19, 1H, *p*-phenyl-C*H*), 7.45 (10, 6H, Tp*-C*H*), 7.75 (33, 1H, cyclohexadiene-C*H*), 8.37 (840, 2H, Tp*-B*H*), 10.51 (t, 2H, *p*-phenyl-C*H*, *J* = 6.2 Hz), 10.78 (14, 4H, *o*/*m*-phenyl-C*H*), 15.15 (104, 2H, cyclohexadiene-C*H*), 21.72 (39, 4H, *o*/*m*-phenyl-C*H*). ^{11}B NMR (C$_6$D$_6$, 25 °C): δ (ppm) = 7.2. ^{31}P NMR (C$_6$D$_6$, 25 °C): δ (ppm) = 84.77. IR (KBr): ν_{B-H} = 2553, 2526 cm^{-1}. **2-^{i}Pr:** Elemental analysis of $C_{58}H_{72}B_2N_{12}OPU$, Calculated: C, 56.00; H, 5.83; N, 13.51. Found: C, 55.52; H, 5.81; N, 13.89. ^{1}H NMR (C$_6$D$_6$, 25 °C): δ (ppm) = −16.12 (63, 18H, Tp*-C*H*$_3$), 0.62 (6, 24H, Tp*-C*H*$_3$ + ^{i}Pr-C*H*$_3$), 1.94 (8, d, 2H, benzyl C*H*$_2$, *J* = 5.6 Hz), 2.16 (m, 1H, *i*Pr-C*H*), 5.42 (16, 2H, cyclohexadiene-C*H*), 6.12 (d, 2H, benzyl-*m*-C*H*, *J* = 8.0 Hz), 6.24 (6, 2H, benzyl-*o*-C*H*, *J* = 8.1 Hz), 7.45 (12, 6H, Tp*-C*H*), 7.73 (23, 1H, cyclohexadiene-C*H*), 8.51 (130, 2H, Tp*-B*H*), 10.54 (t, 2H, *p*-phenyl-C*H*, *J* = 6.3 Hz), 10.81 (d, 4H, *o*/*m*-phenyl-C*H*, *J* = 6.0 Hz), 15.20 (99, 2H, cyclohexadiene-C*H*), 21.80 (53, 4H, *o*/*m*-phenyl-C*H*). ^{11}B NMR (C$_6$D$_6$, 25 °C): δ (ppm) = 7.1. ^{31}P NMR (C$_6$D$_6$, 25 °C): δ (ppm) = 83.78. IR (KBr): ν_{B-H} = 2552, 2524 cm^{-1}. **2-^{t}Bu**: Due to the presence of small amounts of Tp*$_2$UI in this compound, reliable elemental analysis was not possible. This species does not affect the overall outcome of the reaction. ^{1}H NMR (C$_6$D$_6$, 25 °C): δ (ppm) = −16.06 (65, 18H, Tp*-C*H*$_3$), 0.62 (7, 18H, Tp*-C*H*$_3$), 0.72 (s, 9H, *t*Bu-C*H*$_3$), 1.98 (d, 2H, benzyl-C*H*$_2$, J = 6.4 Hz), 5.41 (12, 2H, cyclohexadiene-C*H*), 6.18 (12, 2H, benzyl-*o*/*m*-C*H*, J = 8.2 Hz), 6.42 (d, 2H, benzyl-*o*/*m*-C*H*, J = 8.2 Hz), 7.44 (44, 6H, Tp*-C*H*), 8.42 (5, Tp*-B*H*), 10.53 (17, 2H, *p*-phenyl-C*H*, J = 6.3 Hz), 10.80 (d, 4H, *o*/*m*-phenyl-C*H*, *J* = 6.0 Hz), 15.18 (60, 2H, cyclohexadiene-C*H*), 21.75 (184, 4H, *o*/*m*-phenyl-C*H*). ^{11}B NMR (C$_6$D$_6$, 25 °C): δ (ppm) = 6.8. ^{31}P NMR (C$_6$D$_6$, 25 °C): δ (ppm) = 83.28. IR (KBr): $\nu_{B-H=}$ 2550, 2519 cm^{-1}. **2-OMe**: Elemental analysis of $C_{56}H_{68}B_2N_{12}OPU$, Calculated: C, 55.32; H, 5.64, N, 13.82. Found: C, 53.9; H, 5.77; N, 13.31. Reliable elemental analysis of this compounds was not possible, likely a result of incomplete combustion. ^{1}H NMR (C$_6$D$_6$, 25 °C): δ (ppm) = −16.04 (548, 18H, Tp*-C*H*$_3$), 0.61 (6, 18H, Tp*-C*H*$_3$) 1.99 (12, d, 2H, benzyl-C*H*$_2$), 2.64 (2, 3H, benzyl-*m*-OC*H*$_3$), 5.44 (399, 2H, cyclohexadiene-C*H*), 5.84 (6, 2H, benzyl-*m*-C*H*), 6.08 (6, 2H, benzyl-*o*-C*H* + benzyl-*o*/*p*-C*H*), 6.17 (15, 1H, cyclohexadiene-C*H*), 6.30 (t, 1H, benzyl-*m*-C*H*, *J* = 8.1 Hz) 7.44 (10, 6H, Tp*-C*H*), 8.43 (1306, 2H, Tp*-B*H*), 10.50 (t, 2H, *p*-phenyl-C*H*, *J* = 6.3 Hz), 10.76 (d, 4H, *o*/*m*-phenyl-C*H*, *J* = 6.0 Hz), 15.16 (49, 2H, cyclohexadiene-C*H*), 21.68 (39, 4H, *o*/*m*-phenyl-C*H*). ^{11}B NMR (C$_6$D$_6$, 25 °C): δ (ppm) = 7.4. ^{31}P NMR (C$_6$D$_6$, 25 °C): δ (ppm) = 84.71. IR (KBr): ν_{B-H} = 2552, 2524 cm^{-1}.

Synthesis of Tp*$_2$U[OP(*p*-tolyl)$_2$(C$_6$H$_4$(CH$_3$)CH$_2$C$_6$H$_5$)] (3-tolyl). To a 20 mL scintillation vial, **1-Bn** (0.300 g, 0.325 mmol) was dissolved in 7 mL of THF. In a separate vial, OP(*p*-tolyl)$_3$ (0.104 g, 0.325 mmol) was dissolved in 3 mL of THF. The phosphine oxide was added to the stirring green benzyl solution, and a color change was seen within 25 min to brown. After an additional 60 min, volatiles were removed *in vacuo*, affording a brown powder. The crude product was washed with *n*-pentane (3 × 2 mL) and dried, yielding a brown powder (0.387 g, 0.314 mmol, 97%) assigned as Tp*$_2$U[OP(*p*-tolyl)$_2$(C$_6$H$_4$(CH$_3$)CH$_2$C$_6$H$_5$)] (**3-tolyl**). ^{1}H NMR (C$_6$D$_6$, 25 °C): δ (ppm) = −16.19 (89, 18H, Tp*-C*H*$_3$), 0.76 (7, 18H, Tp*-C*H*$_3$), 0.79 (d, 6H, tolyl-C*H*$_3$, *J* = 7.6 Hz), 1.94 (2, 2H, benzyl C*H*$_2$), 4.26 (d, 6H, tolyl-C*H*$_3$), 5.33 (d, 2H, cyclohexadiene-C*H*, *J* = 6.8 Hz), 6.50 (m, 3H, benzyl-*o*/*m*-C*H* and benzyl-*p*-C*H*), 6.70 (d, 2H, benzyl-*o*/*m*-C*H*, *J* = 5.9 Hz), 7.45 (12, 6H, Tp*-C*H*), 8.77 (2, Tp*-B*H*), 10.70 (8, 2H, *p*-phenyl-C*H*), 10.71 (14, 4H, *o*/*m*-phenyl-C*H*), 15.27 (21, 2H, cyclohexadiene-C*H*), 21.56 (42, 4H, *o*/*m*-phenyl-C*H*). 11B NMR (C$_6$D$_6$, 25 °C): δ (ppm) = 7.76. 31P NMR (C$_6$D$_6$, 25 °C): δ (ppm) = 86.52. Elemental analysis of $C_{58}H_{72}B_2N_{12}OUP$, Calculated: C 56.00; H 5.83; N 13.51. Found: 54.97; H 5.67; N 12.37. Reliable elemental analysis of this compounds was not possible, likely a result of incomplete combustion.

■ ASSOCIATED CONTENT

Supporting Information

The Supporting Information is available free of charge on the ACS Publications website at DOI: 10.1021/acs.organomet.7b00896.

General considerations; synthesis of **4-THF**; single crystal determinations, reaction scheme for the synthesis of **4-THF**; molecular structure of **4-THF**; electronic absorption spectra for **4-THF**; IR spectra of **4-THF**, **2-Ph**, **2-^{i}Pr**, **2-^{t}Bu**, **2-OMe**, and **3-tolyl**; ^{1}H NMR spectra of **4-THF**, **2-Ph**, **2-*i*Pr**, **2-^{t}Bu**, **2-OMe**, and **3-tolyl**; COSY spectra of **2-Ph**, **2-^{i}Pr**, and **2-OMe**; ^{11}B NMR spectra of **2-Ph**, **2-^{i}Pr**, **2-^{t}Bu**, **2-OMe**, and **3-tolyl**; ^{31}P spectra of **2-Ph**, **2-^{i}Pr**, **2-^{t}Bu**, **2-OMe**, **3-tolyl**, and OPPh$_3$; crystallographic details for **2-Ph**, **2-^{i}Pr**, **2-OMe**, **4-THF** (PDF)

Accession Codes

CCDC 1587804, 1587807, 1587812, and 1587813 contain the supplementary crystallographic data for this paper. These data can be obtained free of charge via www.ccdc.cam.ac.uk/data_request/cif, or by emailing data_request@ccdc.cam.ac.uk, or by contacting The Cambridge Crystallographic Data Centre, 12 Union Road, Cambridge CB2 1EZ, UK; fax: +44 1223 336033.

■ AUTHOR INFORMATION

Corresponding Author

*E-mail: sbart@purdue.edu.

ORCID

Caleb J. Tatebe: 0000-0002-7817-388X

Suzanne C. Bart: 0000-0002-8918-9051

Author Contributions

†These authors contributed equally.

Notes

The authors declare no competing financial interest.

■ ACKNOWLEDGMENTS

The authors gratefully acknowledge a grant from the National Science Foundation (CHE-1665170, SCB). The X-ray crystallographic data in this work was obtained on instruments funded by the National Science Foundation through the Major Research Instrumentation Program (CHE-1625543). The authors also acknowledge Professor Gregory C. Ferrence (Illinois State University) for the use of their single crystal X-ray diffractometer (funded by NSF: CHE-1039689) for **2-Ph** and Dr. John S. Harwood for assistance in 2D NMR experiments. Purdue University's Summer Undergraduate Research Fellowship (SURF) is also acknowledged for financial support (Z.T.).

■ REFERENCES

(1) Walsh, P. J.; Hollander, F. J.; Bergman, R. G. *Organometallics* **1993**, *12*, 3705−3723.

(2) Etter, M. C.; Baures, P. W. *J. Am. Chem. Soc.* **1988**, *110*, 639−640.

(3) Jones, M. B.; Gaunt, A. J. *Chem. Rev.* **2013**, *113*, 1137−1198.

DOI: 10.1021/acs.organomet.7b00896
Organometallics 2018, 37, 934−940

(4) Liddle, S. T. *Angew. Chem., Int. Ed.* **2015**, *54*, 8604−8641.
(5) Schelter, E. J.; Wu, R.; Scott, B. L.; Thompson, J. D.; Morris, D. E.; Kiplinger, J. L. *Angew. Chem., Int. Ed.* **2008**, *47*, 2993−2996.
(6) Lam, O. P.; Feng, P. L.; Heinemann, F. W.; O'Connor, J. M.; Meyer, K. *J. Am. Chem. Soc.* **2008**, *130*, 2806−2816.
(7) Kraft, S. J.; Fanwick, P. E.; Bart, S. C. *Inorg. Chem.* **2010**, *49*, 1103−1110.
(8) Kiernicki, J. J.; Newell, B. S.; Matson, E. M.; Anderson, N. H.; Fanwick, P. E.; Shores, M. P.; Bart, S. C. *Inorg. Chem.* **2014**, *53*, 3730−3741.
(9) Lam, O. P.; Anthon, C.; Heinemann, F. W.; O'Connor, J. M.; Meyer, K. *J. Am. Chem. Soc.* **2008**, *130*, 6567−6576.
(10) Mullane, K. C.; Cheisson, T.; Nakamaru-Ogiso, E.; Manor, B. C.; Carroll, P. J.; Schelter, E. J. *Chem. - Eur. J.* **2018**, *24*, 826−837.
(11) Matson, E. M.; Forrest, W. P.; Fanwick, P. E.; Bart, S. C. *J. Am. Chem. Soc.* **2011**, *133*, 4948−4954.
(12) Matson, E. M.; Kiernicki, J. J.; Anderson, N. H.; Fanwick, P. E.; Bart, S. C. *Dalton Trans.* **2014**, *43*, 17885−17888.
(13) Tatebe, C. J.; Johnson, S. A.; Zeller, M.; Bart, S. C. *J. Organomet. Chem.* **2017**, DOI: 10.1016/j.jorganchem.2017.09.013.
(14) Pangborn, A. B.; Giardello, M. A.; Grubbs, R. H.; Rosen, R. K.; Timmers, F. J. *Organometallics* **1996**, *15*, 1518−1520.
(15) Johnson, S. A.; Kiernicki, J. J.; Fanwick, P. E.; Bart, S. C. *Organometallics* **2015**, *34*, 2889−2895.
(16) Busacca, C. A.; Raju, R.; Grinberg, N.; Haddad, N.; James-Jones, P.; Lee, H.; Lorenz, J. C.; Saha, A.; Senanayake, C. H. *J. Org. Chem.* **2008**, *73*, 1524−1531.
(17) Mansell, S. M.; Kaltsoyannis, N.; Arnold, P. L. *J. Am. Chem. Soc.* **2011**, *133*, 9036−9051.
(18) Hoerger, C. J.; La Pierre, H. S.; Maron, L.; Scheurer, A.; Heinemann, F. W.; Meyer, K. *Chem. Commun.* **2016**, *52*, 10854−10857.
(19) Evans, W. J.; Traina, C. A.; Ziller, J. W. *J. Am. Chem. Soc.* **2009**, *131*, 17473−17481.
(20) Castro-Rodríguez, I.; Olsen, K.; Gantzel, P.; Meyer, K. *J. Am. Chem. Soc.* **2003**, *125*, 4565−4571.
(21) Matson, E. M.; Fanwick, P. E.; Bart, S. C. *Organometallics* **2011**, *30*, 5753−5762.
(22) Johnson, S. A.; Tatebe, C. J.; Gonzalez, S.; Zeller, M.; Bart, S. C. *Polyhedron* **2017**, *125*, 107−112.
(23) Antunes, M. A.; Domingos, Â.; Santos, I. C.; Marques, N.; Takats, J. *Polyhedron* **2005**, *24*, 3038−3045.
(24) Maria, L.; Domingos, Â.; Galvão, A.; Ascenso, J.; Santos, I. C. *Inorg. Chem.* **2004**, *43*, 6426−6434.
(25) Maier, R.; Müller, J.; Kanellakopulos, B.; Apostolidis, C.; Domingos, A.; Marques, N.; De Matos, A. P. *Polyhedron* **1993**, *12*, 2801−2808.
(26) Brennan, J. G.; Andersen, R. A.; Zalkin, A. *Inorg. Chem.* **1986**, *25*, 1761−1765.
(27) Maria, L.; Campello, M. P.; Domingos, Â.; Santos, I.; Andersen, R. A. *J. Chem. Soc., Dalton Trans.* **1999**, 2015−2020.
(28) Antunes, M. A.; Ferrence, G. M.; Domingos, Â.; McDonald, R.; Burns, C. J.; Takats, J.; Marques, N. *Inorg. Chem.* **2004**, *43*, 6640−6643.
(29) Sun, Y.; McDonald, R.; Takats, J.; Day, V. W.; Eberspacher, T. A. *Inorg. Chem.* **1994**, *33*, 4433−4434.
(30) Gorobets, E.; Parvez, M.; Keay, B. *Synlett* **2008**, *2008*, 129−133.
(31) Matson, E. M.; Kiernicki, J. J.; Fanwick, P. E.; Bart, S. C. *Eur. J. Inorg. Chem.* **2016**, *2016*, 2527−2533.
(32) Clark, C. L.; Lockhart, J. J.; Fanwick, P. E.; Bart, S. C. *Chem. Commun.* **2015**, *51*, 14084−14087.
(33) Matson, E. M.; Breshears, A. T.; Kiernicki, J. J.; Newell, B. S.; Fanwick, P. E.; Shores, M. P.; Walensky, J. R.; Bart, S. C. *Inorg. Chem.* **2014**, *53*, 12977−12985.
(34) Matson, E. M.; Forrest, W. P.; Fanwick, P. E.; Bart, S. C. *Organometallics* **2012**, *31*, 4467−4473.
(35) Kraft, S. J.; Walensky, J. R.; Fanwick, P. E.; Hall, M. B.; Bart, S. C. *Inorg. Chem.* **2010**, *49*, 7620−7622.
(36) Kepp, K. P. *Inorg. Chem.* **2016**, *55*, 9461−9470.
(37) Matson, E. M.; Forrest, W. P.; Fanwick, P. E.; Bart, S. C. *Organometallics* **2013**, *32*, 1484−1492.

DOI: 10.1021/acs.organomet.7b00896
Organometallics 2018, 37, 934−940